Neuro-Oncology Advances

3(1), 1–13, 2021 | https://doi.org/10.1093/noajnl/vdab179 | Advance Access date 01 December 2021

Phase I study using crenolanib to target PDGFR kinase in children and young adults with newly diagnosed DIPG or recurrent high-grade glioma, including DIPG

Christopher L. Tinkle, Alberto Broniscer, Jason Chiang, Olivia Campagne, Jie Huang, Brent A. Orr, Xiaoyu Li, Zoltan Patay, Jinghui Zhang, Suzanne J. Baker, Thomas E. Merchant, Vinay Jain, Arzu Onar-Thomas, Clinton F. Stewart, Cynthia Wetmore†, and Amar Gajjar†

Department of Radiation Oncology, St. Jude Children's Research Hospital, Memphis, Tennessee, USA (C.L.T., T.E.M.); Department of Oncology, St. Jude Children's Research Hospital, Memphis, Tennessee, USA (A.B., C.W., A.G.); Department of Pathology, St. Jude Children's Research Hospital, Memphis, Tennessee, USA (J.C., B.A.O., X.L.); Department of Pharmaceutical Sciences, St. Jude Children's Research Hospital, Memphis, Tennessee, USA (O.C., C.F.S.); Department of Biostatistics, St. Jude Children's Research Hospital, Memphis, Tennessee, USA (J.H., A.O.-T.); Department of Diagnostic Imaging, St. Jude Children's Research Hospital, Memphis, Tennessee, USA (Z.P.); Department of Computational Biology, St. Jude Children's Research Hospital, Memphis, Tennessee, USA (J.Z.); Department of Developmental Neurobiology, St. Jude Children's Research Hospital, Memphis, Tennessee, USA (S.J.B.); Arog Pharmaceuticals, Inc., Dallas, Texas, USA (V.J.); Neoleukin Therapeutics, Inc., Seattle, Washington, USA (C.W.)

Present affiliation: Department of Pediatrics, University of Pittsburgh Medical Center, Pittsburgh, Pennsylvania, USA (A.B.)

†*These authors contributed equally as cosenior authors.*

Corresponding Author: Christopher L. Tinkle, MD, PhD, Department of Radiation Oncology, St. Jude Children's Research Hospital, 262 Danny Thomas Place, MS 210, Memphis, TN 38105-3678, USA (christopher.tinkle@stjude.org).

Abstract

Background. Platelet-derived growth factor receptor (PDGFR) signaling has been directly implicated in pediatric high-grade gliomagenesis. This study evaluated the safety and tolerability of crenolanib, a potent, selective inhibitor of PDGFR-mediated phosphorylation, in pediatric patients with high-grade glioma (HGG).

Methods. We used a rolling-6 design to study the maximum tolerated dose (MTD) of once-daily crenolanib administered during and after focal radiation therapy in children with newly diagnosed diffuse intrinsic pontine glioma (DIPG) (stratum A) or with recurrent/progressive HGG (stratum B). Pharmacokinetics were studied during the first cycle at the first dose and at steady state (day 28). Alterations in *PDGFRA* were assessed by Sanger or exome sequencing and interphase fluorescence in situ hybridization or single nucleotide polymorphism arrays.

Results. Fifty evaluable patients were enrolled in the 2 strata, and an MTD of 170 mg/m^2 was established for both. Dose-limiting toxicities were primarily liver enzyme elevations and hematologic count suppression in both strata. Crenolanib $AUC_{0–48h}$ and C_{MAX} did not differ significantly for crushed versus whole-tablet administration. Overall, *PDGFRA* alterations were observed in 25% and 30% of patients in stratum A and B, respectively. Neither crenolanib therapy duration nor survival outcomes differed significantly by *PDGFRA* status, and overall survival of stratum A was similar to that of historical controls.

Conclusions. Children tolerate crenolanib well at doses slightly higher than the established MTD in adults, with a toxicity spectrum generally similar to that in adults. Studies evaluating intratumoral PDGFR pathway inhibition in biomarker-enriched patients are needed to evaluate further the clinical utility of crenolanib in this population.

Key Points

- Crenolanib has similar pharmacokinetics, irrespective of whole-tablet or crushed-tablet administration, and an acceptable safety profile.
- Neither a correlation with PDGFRA alterations and outcomes nor a preliminary signal of efficacy was observed.

Importance of the Study

Aberrant activation of the platelet-derived growth factor (PDGF) pathway occurs in ~30% of pediatric high-grade glioma (HGG), and the PDGF receptor α (*PDGFRA*) gene has been directly implicated in pediatric gliomagenesis. We evaluated the safety, tolerability, pharmacokinetics, and efficacy of crenolanib, a potent, selective inhibitor of PDGFR-mediated phosphorylation, combined with radiation therapy or as single-agent therapy for patients with newly diagnosed DIPG or recurrent HGG, respectively. This first-in-pediatrics phase I study showed that crenolanib exhibits similar pharmacokinetics after whole-tablet or crushed-tablet administration and demonstrates an acceptable safety profile with a toxicity spectrum generally similar to that in adults. In this unselected, primarily clinically diagnosed population, neither a correlation with *PDGFRA* alterations and outcomes nor a preliminary signal of efficacy was observed, suggesting that additional experimental data are needed to better define biomarkers of response and rational combination therapy to support further clinical investigation of crenolanib in pHGG.

Aberrant activation of platelet-derived growth factor receptor (PDGFR) signaling is common in pediatric high-grade glioma (pHGG) and has been directly implicated in driving pediatric glioma formation in vivo.[1–5] The *PDGFRA* gene, which encodes PDGFRα, is the most commonly altered receptor tyrosine kinase (RTK) gene in both pediatric non-brainstem HGG and diffuse intrinsic pontine glioma (DIPG).[2,6,7] Genetic alterations including gene amplification, mutation, or both have been noted in approximately 20–30% of pHGG, and they are most commonly subclonal and heterogeneous, with some tumor cells co-amplifying multiple RTK genes or discrete cell populations within the same tumor amplifying different RTK genes.[6,8–10] Although the heterogeneity of *PDGFRA* alterations and redundant RTK signaling in pHGG might limit the efficacy of single-agent selective RTK inhibitors, the growth advantage conferred by overexpression of wild-type or mutant PDGFRα was reduced after treatment with the ATP-competitive inhibitors crenolanib and dasatinib,[2] and *PDGFRA* deletion reduced viability in models of H3 K27M glioma.[3]

Crenolanib is a potent and selective oral inhibitor of PDGFR and FMS-like tyrosine kinase (FLT3)-mediated phosphorylation of tyrosine substrates, with 50% inhibitory concentrations of approximately 1 ng/mL (2.25 nM) and 0.4 ng/mL (0.902 nM) for the PDGF α and β receptor types, respectively.[11–13] Preliminary studies of the central nervous system (CNS) penetration of systemically administered crenolanib have been conducted in a murine model of HGG, using microdialysis probes placed directly into the tumor tissue.[14] With this approach, crenolanib concentrations in tumor extracellular fluid were ~63% of unbound plasma concentrations.[14] In the C6 glioblastoma xenograft model, a single oral dose of 10 mg/kg resulted in 53% inhibition of phospho-PDGFR that was maintained for 3 h, whereas crenolanib resulted in 47% inhibition of human glioma xenograft (U87MG) growth after 9 days of dosing at 50 mg/kg BID, which corresponded to plasma concentrations of 100 ng/mL (Crenolanib Investigator's Brochure, AROG Pharmaceuticals, LLC, 2011). A phase I dose-escalation study of crenolanib in adults with recurrent solid tumors established a recommended phase II dosage of 200 mg once daily when the drug was administered as an uncoated tablet taken without food, while a maximum tolerated dose (MTD) was not reached when crenolanib was administered as uncoated tablets with food.[11] Dose-limiting toxicities (DLTs) included hematuria, increased aspartate aminotransferase (AST) or alanine aminotransferase (ALT), insomnia, and nausea/vomiting. Most treatment-related adverse events (AEs) were of grade 1 or 2 severity; they included nausea, vomiting, fatigue, and diarrhea. While recent studies have explored targeted inhibition of PDGFR signaling in pHGG, including imatinib mesylate[15] and dasatinib,[16,17] the pharmacokinetic and pharmacodynamic properties of crenolanib suggest that this agent may represent a more CNS penetrant and potent and selective inhibitor of PDGFR α and β.[11,14,18–21]

These data provide the rationale to investigate crenolanib for treating pHGG, including DIPG. The primary objectives of this study were to estimate the MTD of crenolanib administered concurrently with radiation therapy (RT) in patients with newly diagnosed DIPG and as a single agent in patients with progressive or recurrent

pHGG and to characterize the pharmacokinetic properties of crenolanib in pediatric patients. We also aimed to describe the toxicities associated with crenolanib in this population and to evaluate alterations in *PDGFRA* in available tumor samples and correlate with treatment duration and clinical outcome. Finally, through an expansion cohort of patients treated at the pediatric MTD, we sought to evaluate the preliminary antitumor activity of crenolanib in pHGG.

Materials and Methods

Patients

Patients between 18 months and 21 years of age with newly diagnosed DIPG or other high-grade brainstem glioma (stratum A) or with recurrent, refractory, or progressive HGG (WHO grade III/IV) or DIPG (stratum B) were eligible for this study. For patients with radiologic features of DIPG, histologic confirmation was not required. Other eligibility criteria are detailed in Supplementary Material.

The study protocol was approved by our institutional review board before initial patient enrollment, and continuing approval was maintained throughout the study. Written informed consent for participation was obtained from patients' parents or legal guardians, and assents were obtained when appropriate. The study was registered on ClinicalTrials.gov (NCT01393912).

Study Design, Treatment Plan, and Study Evaluations

This was an open-label, single-institution, phase I dose-escalation study using a rolling-6 design. The MTD was defined as the highest dosage at which no more than one of 6 evaluable patients experienced a DLT. DLTs attributable to the study drug are detailed in Supplementary Material. Toxicities were graded based on the National Cancer Institute Common Toxicity Criteria for Adverse Events (version 4.0). The DLT evaluation period consisted of the first 8 weeks of therapy for patients enrolled in stratum A and the first 4 weeks for patients enrolled in stratum B.

Crenolanib was administered orally daily for 28 consecutive days, which defined one cycle. For both strata, crenolanib treatment was planned for a maximum of 5 dosage levels (Supplementary Figure 1), with independent dose escalation for each stratum. The initial dosage of crenolanib was 100 mg/m^2, which was approximately 80% of the adult MTD when administered as uncoated tablets without food,[11] and one lower dosage level was also provided in case the starting level was deemed too toxic. The maximum planned duration of crenolanib administration was 2 years. Crenolanib was administered with food as uncoated tablets of 20 mg and 100 mg. The dose was rounded to the nearest 20 mg. The delivered crenolanib dose was calculated based on the BSA before the start of the study therapy and before each crenolanib cycle. Additional details of crenolanib administration as intact or crushed tablets and supportive care are described in Supplementary Material.

For stratum A, RT and crenolanib were started on the same day and crenolanib was continued daily during and after RT (without a break). Three-dimensional conformal RT was delivered as 1.8-Gy fractions once daily, 5 days a week, for a cumulative dose of 54 Gy. Radiotherapy guidelines and study evaluations are further detailed in Supplementary Material.

Pharmacokinetic Studies

Pharmacokinetic studies were conducted in all patients during cycle 1 of crenolanib therapy to characterize the disposition of crenolanib in serum. Single-dose blood samples were collected predose and at 1, 2, 4, 8 (±2), 24 (±6), and 48 (±6) h after the first crenolanib dose on day 1. The crenolanib dose on day 2 was held for the pharmacokinetic studies. Steady-state blood samples were collected predose and at 1, 2, 4, 8 (±2), and 24 (±6) h postdose on day 28. Additional trough samples were collected before the crenolanib dose weekly for 2 consecutive weeks on days 14 and 21 of cycle 1. Each blood sample (2 mL) was collected in a labeled red-top tube and centrifuged for 10 min at 4°C at 1500 × *g*. The extracted serum was stored at –80°C within 1 h of collection. Optional pharmacokinetic studies were performed in consenting patients to determine the crenolanib disposition in cerebrospinal fluid (CSF). Single or serial CSF samples were collected in patients with access to CSF, along with a simultaneous serum sample, if possible. Serum and CSF crenolanib concentrations were determined as described and further detailed in Supplementary Material.[22]

The impact on relative drug bioavailability of crushing the crenolanib tablet in applesauce versus taking a whole tablet was evaluated by comparing the crenolanib $AUC_{0–48h}$ and C_{MAX} values after the first dose among the first 6 patients taking crenolanib as whole tablets (stratum A1) and the 6 patients taking crenolanib as crushed tablets (stratum A2), using the Mann–Whitney test.

Histopathology and Molecular Analysis

Histopathology was centrally reviewed by a neuropathologist specializing in pediatric CNS tumors (J.C.). Standard hematoxylin and eosin histopathologic preparations from each case were supplemented by immunohistochemistry on 5-μm formalin-fixed, paraffin-embedded (FFPE) tissue sections. Monoclonal anti-histone H3 K27M antibody (RevMab Biosciences, #31-1175-00, clone RM192; diluted 1:250) was used to identify tumors expressing K27M-mutant histone H3. A monoclonal antibody (Cell Signaling Technology, #9733, clone C36B11; diluted 1:200) was used to confirm the loss of trimethylation of the histone H3 K27 residue in K27M-mutant tumors. Sanger sequencing of genomic DNA extracted from FFPE tissue was used to identify the mutant histone H3 variant and *PDGFRA* hotspot mutations with the primers listed in Supplementary Table 1. Copy-number variation (CNV) of *PDGFRA* (4q12) was detected by interphase fluorescence in situ hybridization with probes developed in-house, using the following BAC clones: *PDGFRA* (RP11-231C18 + RP11-601I15) with 4p12

control (CTD-2057N12 + CTD-2588A19). Amplification was defined as a gain of more than 5 PDGFRA signals per cell or the presence of double minutes or homogeneously staining regions. In a subset of patients, whole-genome sequencing or whole-exome sequencing was used to identify *PDGFRA* single nucleotide variants (SNVs), and single nucleotide polymorphism arrays were performed to identify *PDGFRA* CNVs as previously described.[6,23] Sequencing results were analyzed using an institutionally established pipeline in a Clinical Laboratory Improvement Amendments (CLIA)–certified laboratory.[23] SNVs were discovered using the Bambino variant-detection program, annotated and ranked by putative pathogenicity, and then manually reviewed.[23]

Statistical Analysis

Progression-free survival (PFS) was defined as the interval between the start of therapy and disease progression or death from any cause, whichever occurred first. Overall survival (OS) was defined as the interval from the date of diagnosis to death from any cause. Patients who experienced no events were censored at the date of the last follow-up. The distribution of OS and PFS was estimated using the Kaplan–Meier method and compared via the log-rank test. The Wilcoxon signed-rank sum test and the sign test were used to analyze paired results from pharmacokinetic studies. In order to study the PK characteristics of a child-friendly administration of the agent, an expansion cohort was incorporated (stratum A2) in which patients received the study agent as a crushed tablet. Spearman correlations were used to assess the association between selected pharmacokinetic parameters. Associations between crenolanib exposure (AUC) values and all AEs of grade 3 or higher that were at least possibly attributable to crenolanib were explored between individual single-dose crenolanib AUC values obtained at day 1 of course 1 and toxicity that occurred within the first 28 days, and between steady-state crenolanib AUC values obtained at day 28 of cycle 1 and toxicity that occurred after the first 28 days. A 2-sided significance level of $P < .05$ was used for all statistical tests. Statistical analyses were conducted using SAS Version 9.4 (SAS Institute).

Results

From July 2011 until December 2013, 32 patients were enrolled in stratum A and 23 were enrolled in stratum B. Supplementary Table 2 lists the patient and treatment characteristics, and Figure 1 shows selected clinicopathologic and genomic features for both strata. Patients in stratum A were administered doses of 100

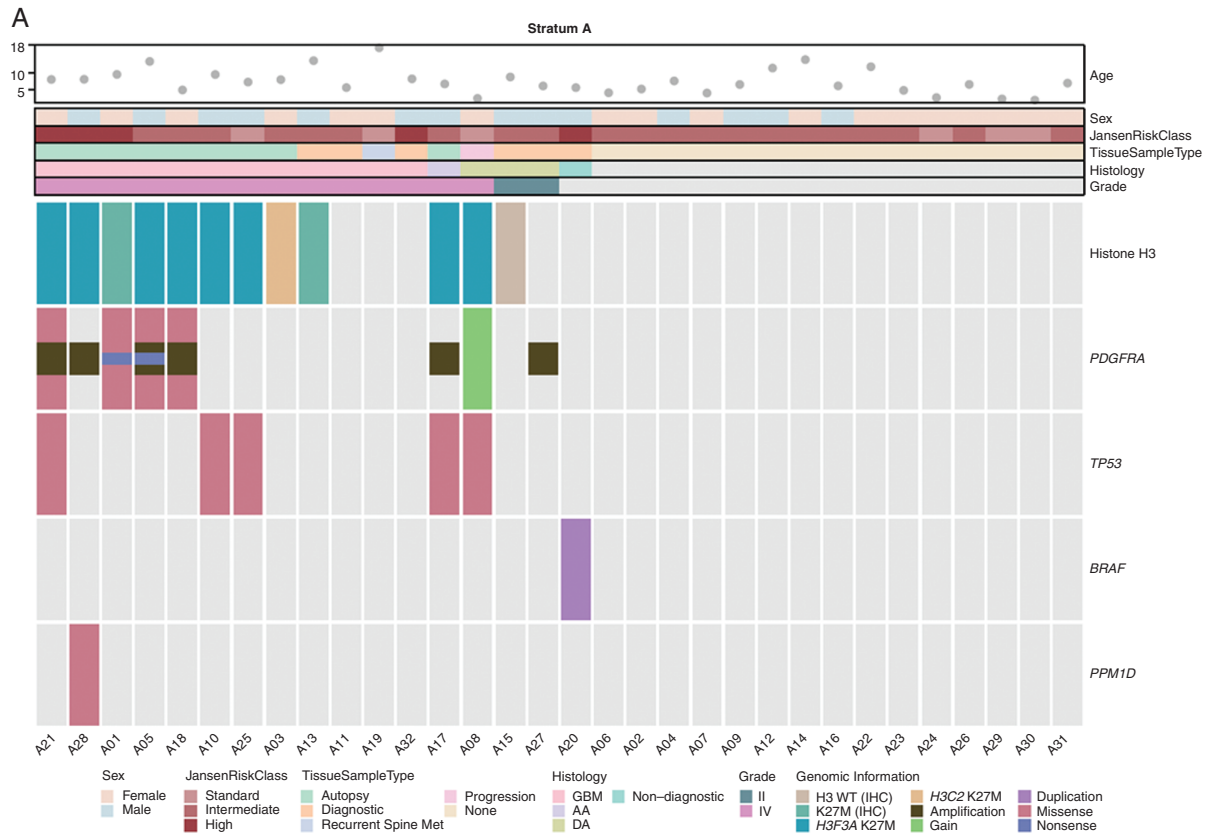

Figure 1. Oncoprint of selected clinical, histologic, and molecular features of patients in (A) stratum A (newly diagnosed DIPG) and

(n = 12), 130 (n = 6), 170 (n = 6), and 220 mg/m^2 (n = 8), corresponding to dosage levels 1–4, respectively, to determine the MTD (Supplementary Figure 1). Patients in stratum B were administered doses of 100 (n = 3), 130 (n = 6), 170 (n = 7), and 220 mg/m^2 (n = 7).

Toxicities

Of the 32 patients in stratum A, 2 (both treated at dose level 4) were considered inevaluable for MTD estimation because treatment was discontinued before completion of the 8-week DLT period for reasons other than toxicity. The following DLTs attributable to crenolanib were noted during the DLT observation period: grade 4 neutropenia (dose level 1), grade 3 gamma-glutamyl transferase (GGT) elevation (dose level 3), grade 3 GGT elevation (dose level 4), and grade 3 ALT elevation (dose level 4). Additional significant toxicities necessitating dose reduction noted beyond the DLT observation period included grade 3 GGT and ALT elevations (dose level 1), grade 3 neutropenia (dose level 1), grade 3 leukopenia (dose level 2), and grade 3 GGT and ALT elevations (dose level 3). One patient experienced recurrently elevated GGT, ultimately necessitating dose reduction from dose level 3 to dose level 1, and one patient was taken off therapy because of recurrent grade 3 neutropenia at dose level 0. The most common grade 3/4 toxicity in stratum A was leukopenia that resolved with drug interruption. Given the observation of a DLT in 2 of 6 evaluable patients treated at dose level 4 during the DLT period, the pediatric MTD for stratum A was determined to be 170 mg/m^2 (dose level 3). Table 1 summarizes the data on toxicities at least possibly attributable to crenolanib for all patients in stratum A during and after the initial 8 weeks of therapy.

Of the 23 patients in stratum B, 3 (1 treated at dose level 3, 2 treated at dose level 4) were considered inevaluable for MTD estimation because treatment was discontinued before completion of the 4-week DLT period for reasons other than toxicity. The following DLTs attributable to crenolanib were noted during the DLT observation period: grade 4 GGT, ALT, and AST elevations (dose level 3); grade 3 amylase, GGT, ALT, and AST elevations (dose level 4); and grade 3 GGT elevation (dose level 4). The most common grade 3/4 toxicity in stratum B was leukopenia that resolved with drug interruption. Given the observation of a DLT in 2 of 5 evaluable patients treated at dose level 4 during the DLT period, the pediatric MTD for stratum B was also determined to be 170 mg/m^2 (dose level 3). Supplementary Table 3 summarizes toxicities at least possibly attributable to crenolanib for all patients enrolled in stratum B during and after the initial 4 weeks of therapy.

The median duration of treatment for stratum A was 179 days (range, 24–726 days), and the median number of

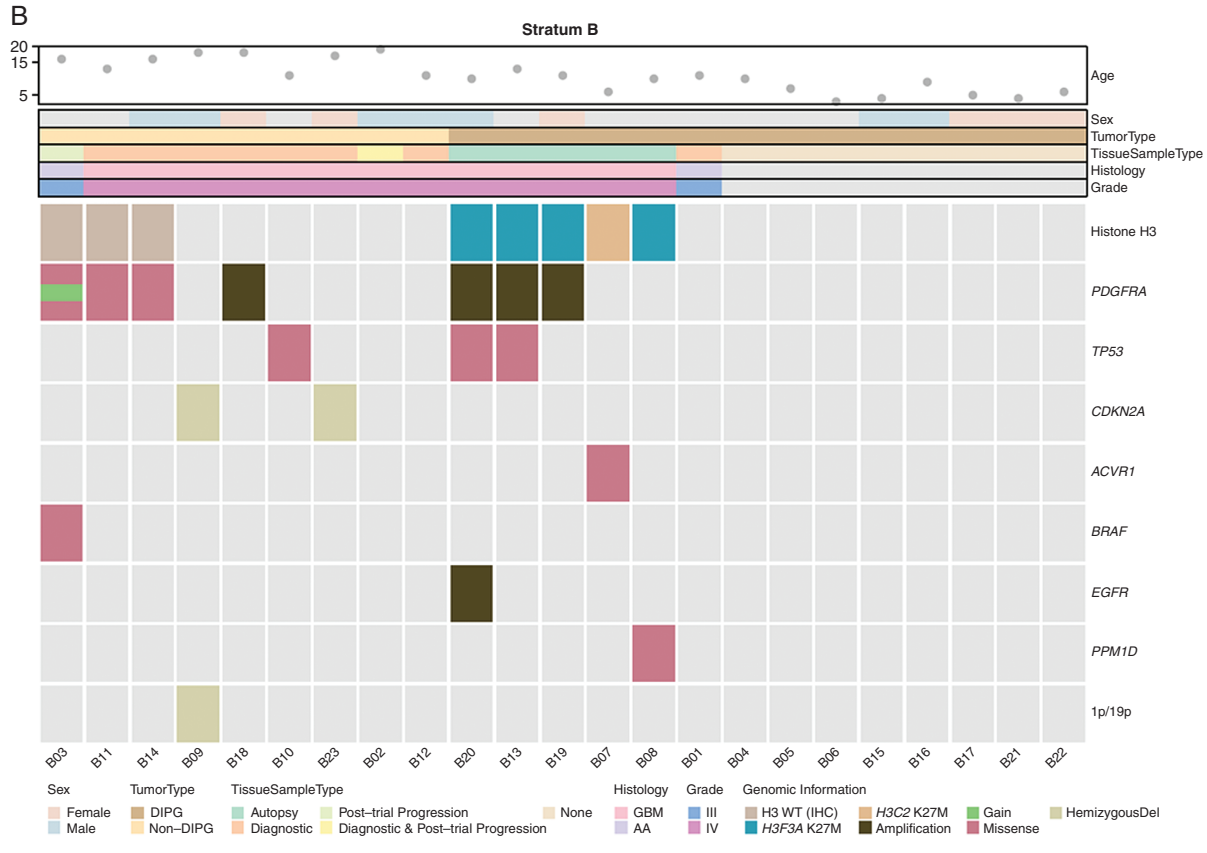

Figure 1. (cont.) (B) stratum B (recurrent HGG, including DIPG).

Table 1. Most Significant Toxicities Attributed to Crenolanib During and After the DLT Evaluation Period in Patients With Newly Diagnosed DIPG (stratum A)

	Level 1		Level 2		Level 3		Level 4	
	n = 12		n = 6		n = 6		n = 8	
	Grade 1/2	Grade 3/4	Grade 1/2	Grade 3/4	Grade 1/2	Grade 3/4	Grade 1/2	Grade 3/4
Hematologic adverse events								
Lymphocyte count decreased	2 (17%)	8 (67%)	0	6 (100%)	2 (33%)	4 (67%)	0	8 (100%)
Neutrophil count decreased	0	5 (42%)[a]	1 (17%)	2 (33%)	1 (17%)	0	1 (13%)	0
White blood cell decreased	4 (33%)	5 (42%)	3 (50%)	2 (33%)	4 (67%)	1 (17%)	7 (88%)	0
Platelet count decreased	4 (33%)	1 (8%)	3 (50%)	0	2 (33%)	0	3 (38%)	0
Anemia	3 (25%)	1 (8%)	3 (50%)	0	3 (50%)	0	6 (75%)	0
Nonhematologic adverse events								
ALT increased	10 (83%)	1 (8%)	2 (33%)	2 (33%)	4 (67%)	2 (33%)	6 (75%)	2 (25%)[a]
GGT increased	5 (42%)	3 (25%)	5 (83%)	0	4 (67%)	2 (33%)[a]	6 (75%)	1 (13%)[a]
AST increased	6 (50%)	0	4 (67%)	0	5 (83%)	1 (17%)	7 (88%)	0
Proteinuria	4 (33%)	1 (8%)	5 (83%)	1 (17%)	5 (83%)	0	5 (63%)	0
Hypophosphatemia	7 (58%)	0	3 (50%)	0	3 (50%)	0	6 (75%)	1 (13%)
Hypoalbuminemia	7 (58%)	0	2 (33%)	0	4 (67%)	0	6 (75%)	0
Hypokalemia	5 (42%)	1 (8%)	1 (17%)	1 (17%)	2 (33%)	2 (33%)	3 (38%)	2 (25%)
Serum amylase increased	4 (33%)	2 (17%)	0	1 (17%)	3 (50%)	0	3 (38%)	0
Hypermagnesemia	3 (25%)	0	1 (17%)	0	3 (50%)	0	5 (63%)	0
Lipase increased	5 (42%)	2 (17%)	2 (33%)	0	1 (17%)	0	2 (25%)	0
Hematuria	3 (25%)	0	2 (33%)	0	3 (50%)	0	2 (25%)	0
Hypocalcemia	1 (8%)	0	2 (33%)	0	1 (17%)	0	3 (38%)	1 (13%)
Alkaline phosphatase increased	1 (8%)	0	3 (50%)	0	2 (33%)	0	1 (13%)	0
Hypernatremia	1 (8%)	0	1 (17%)	0	2 (33%)	0	0	0
Vomiting	8 (67%)	1 (8%)	6 (100%)	0	6 (100%)	0	8 (100%)	0
Nausea	8 (67%)	0	5 (83%)	0	5 (83%)	0	7 (88%)	0
Diarrhea	2 (17%)	0	3 (50%)	0	3 (50%)	0	4 (50%)	0
Abdominal pain	2 (17%)	0	3 (50%)	0	2 (33%)	0	1 (13%)	0
Anorexia	1 (8%)	0	1 (17%)	0	3 (50%)	0	2 (25%)	0
Headache	0	1 (8%)	1 (17%)	1 (17%)	0	0	1 (13%)	0
Dyspepsia	2 (17%)	0	0	0	1 (17%)	0	0	0
Stomach pain	1 (8%)	0	2 (33%)	0	0	0	0	0
Fatigue/lethargy	0	0	0	0	3 (50%)	0	0	0

[a]Dose-limiting toxicity.

cycles of therapy was 7 (range, 1–26 cycles). Two patients in stratum A completed all 26 courses of study therapy. The median duration of treatment for stratum B was 36 days (range, 2–727 days), and the median number of cycles of therapy was 2 (range, 1–26 cycles), with one patient completing all 26 cycles of study therapy.

Pharmacokinetics Studies and Toxicity Associations

Serum pharmacokinetic studies after single-dose crenolanib were performed for 55 patients, of whom 5 were considered inevaluable because of excessive vomiting (n = 1 in stratum B, dose level 2) or missing time points in the terminal phase (one each in stratum A1, dose level 1; in stratum B, dose level 3; in stratum A, dose level 4; and in stratum B, dose level 4). Steady-state serum data were collected from 44 patients, of whom 5 were considered inevaluable because of adherence issues (n = 1 in stratum A2, 100 mg/m^2) or missing time points in the terminal phase (n = 1 in stratum A1, 100 mg/m^2; n = 2 in stratum B, 130 mg/m^2; n = 1 in stratum B, 220 mg/m^2).

Summaries of the single-dose and steady-state pharmacokinetic parameters for patients in strata A and B are given in Table 2 and Supplementary Table 4, respectively, and the concentration–time profiles are depicted in Figure 2. Within 100 and 220 mg/m^2, after single

Table 2. Summary of Crenolanib Pharmacokinetic Parameters for Patients With Newly Diagnosed DIPG (stratum A)

Dosage (mg/m^2)	Subgroup	Day	N	T_{MAX} (h)	C_{MAX} (nM)	[a] AUC_{0-T} (h·nM)	CL/F (L/h/m^2)	Half-life (h)
100	A1	D1	5	4 (2–8)	645 (558–1690)	8683 (4566–15 895)	26.2 (14.3–49.7)	8.5 (6.6–10.9)
		D28	4	6 (2–8)	750 (298–981)	7340 (3551–11 022)	27.5 (17.6–59.9)	4.9 (3.6–8.0)
	A2	D1	6	2 (2–4)	692 (297–2450)	7397 (3759–16 455)	32.9 (11.9–66.6)	6.8 (5.7–12.8)
		D28	5	4 (2–8)	651 (200–1320)	6945 (2774–13 864)	32.6 (14.4–68.0)	5.1 (5.0–8.0)
130		D1	6	2 (1–8)	733 (273–2240)	5951 (2675–15 291)	52.1 (20.6–111)	7.3 (2.2–8.2)
		D28	6	4 (2–8)	1110 (273–1860)	14 212 (3936–19 795)	17.6 (13.9–59.3)	6.1 (3.9–10.8)
170		D1	6	4 (1–8)	1240 (494–1880)	14 989 (6187–25 360)	25.4 (15.0–62.8)	8.5 (6.0–9.2)
		D28	6	3 (1–4)	2010 (1300–4210)	24 522 (12 548–52 999)	13.2 (6.4–27.5)	7.2 (4.4–14.2)
220		D1	7	4 (2–8)	1890 (431–5970)	22 060 (4826–64 870)	21.6 (7.9–98.4)	6.75 (5.4–8.3)
		D28	6	2 (1–8)	2270 (1030–9620)	28 394 (7914–105 521)	13.7 (4.3–60.4)	5.5 (4.5–7.6)

[a]On day 1, AUC_{0-T} corresponds to $AUC_{0-\infty}$. On day 28, AUC_{0-T} corresponds to AUC_{0-24h}.

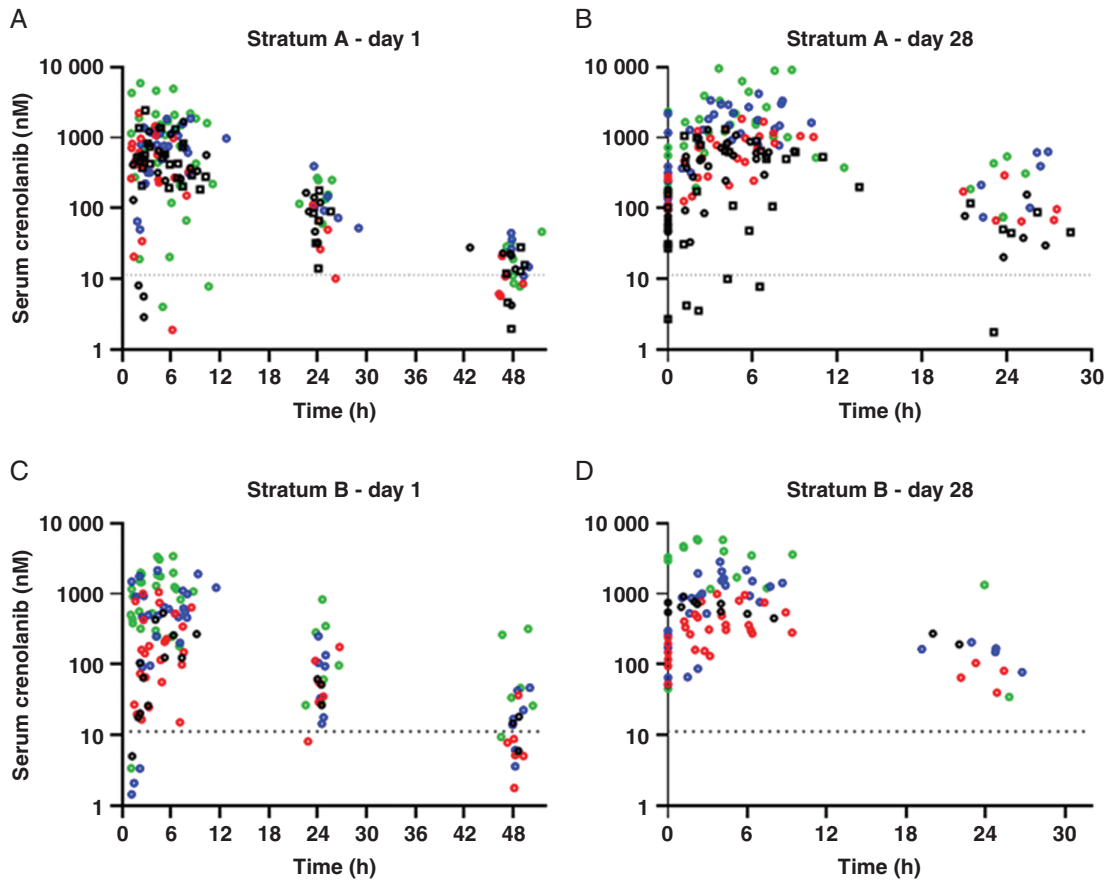

Figure 2. Crenolanib serum concentration–time data in strata A (newly diagnosed DIPG) and B (recurrent HGG) after a single dose on day 1 (A and C) and at steady state on day 28 (B and D). The black, red, blue, and green dots represent individual data for doses of 100, 130, 170, and 220 mg/m^2 of crenolanib, respectively. In panels A and B, the black squares represent data from patients in stratum A2 who took crushed tablets and the black dots represent data from patients in stratum A1 who took whole tablets. In all panels, the dotted line is the lower limit of quantification (5 ng/mL = 11.3 nM).

and multiple doses, crenolanib AUC values appeared to increase with increasing dosages; however, wide interpatient variabilities were observed across dosage levels (Supplementary Figure 2). Crenolanib half-life ranged from 2.2 to 18.8 h across all dosage levels, with a median of 7.1 h. Crenolanib was, overall, absorbed

slowly, with a median (range) T_{MAX} of 4 h (range, 1–8 h) across dosage levels.

The crenolanib AUC_{0-48h} and C_{MAX} of patients in stratum A2 who took crushed tablets in applesauce were not significantly different from those of patients in stratum A1 who took whole tablets ($P = .93$ and $P = .66$, respectively) (Supplementary Figure 3).

CSF crenolanib samples were collected from 2 patients in stratum A2 during the third cycle (one on day 14 and one on day 28, respectively), both approximately 19 h after a crenolanib dose. The CSF crenolanib concentrations were determined as 9.15 and 13.6 nM, respectively. One serum sample was collected simultaneously during the day 28 CSF sampling, revealing a serum crenolanib concentration of 546 nM and a CSF:total serum ratio of 0.025 in that patient.

To investigate potential exposure–toxicity relations, the AUC data were log-transformed to account for the large pharmacokinetic variability. Among the 50 patients with available single-dose crenolanib AUC values, 18 experienced one or more toxicity, as defined previously, within the first 28 days. No association between single-dose crenolanib AUC values and toxicities that occurred within the first 28 days was found (Spearman correlation coefficient = 0.10 with $P = .478$, and Wilcoxon–Mann–Whitney test $P = .507$). Thirty-eight patients had available steady-state crenolanib AUC values and toxicity data, among whom 29 experienced one or more toxicities, as defined previously, after the first 28 days. No association between steady-state crenolanib AUC values and toxicities that occurred after the first 28 days was found (Spearman correlation coefficient = –0.07 with $P = .700$, and Wilcoxon–Mann–Whitney test $P = 1.000$).

Histopathology and Molecular Studies

In stratum A, 17 patients underwent tumor tissue sampling, 6 at diagnostic biopsy, 1 at progression biopsy, 1 at metastatic site progression, and 9 at autopsy (Supplementary Table 2 and Figure 1A). Two of 6 diagnostic biopsies revealed grade 2 diffuse astrocytoma, whereas HGG (grade III/IV) was observed in all other samples. Histone H3 K27M mutation was detected in 11 of 12 samples (91.7%) with sufficient material. *PDGFRA* SNVs were detected in 4 of 10 evaluable samples (40%), with 6 SNVs found in 1 sample, 5 in 1 sample, and 1 in 2 samples each (Supplementary Table 5). The D836Y, D846E, R554S, E556K, and Y849C alterations are predicted to be pathogenic or probably pathogenic,[24,25] the R841* and Y555* alterations truncate the protein kinase domain, and the T230R, I843S, R558P, R558L, and A500T alterations are novel findings. The I843T alteration has been reported previously.[26] *PDGFRA* CNVs were detected in 7 of 15 evaluable samples (46.7%), with copy-number gain noted in one case and amplification in the remainder. In stratum B, 15 patients underwent tumor tissue sampling, 10 before study enrollment, 3 at subsequent progression, and 5 at autopsy, with all samples revealing HGG (Supplementary Table 2 and Figure 1B). Histone H3 K27M mutation was detected in 5 of 10 samples (50%) with sufficient material and was restricted to patients with DIPG (5 of 5 evaluable DIPG cases). *PDGFRA* SNVs were detected in 3 of 10 evaluable samples (30%), with 5 SNVs found in 1 sample, 3 in 1 sample, and 2 in 1 sample (Supplementary Table 5). The H310Q, E311G, S389T, R558P, W559R, K384R, L380R, and A389T alterations are novel findings. *PDGFRA* CNVs were detected in 5 of 13 evaluable samples (38.5%), with copy-number gain noted in one case and amplification in the remainder. The potential impact of *PDGFRA* alterations on the duration of study drug administration was evaluated in a swimmer plot for both strata (Figure 3). When compared to patients harboring tumors without *PDGFRA* SNVs and/or CNVs to those with those aberrations, there were no obvious differences in study treatment duration in either stratum.

Outcomes

Of the 32 patients in stratum A, 2 were lost to follow-up after completion of concurrent crenolanib and RT; one of these patients was ultimately reported to have succumbed to the disease. Twenty-nine patients experienced disease progression, and 30 have died. All patients died of disease except for one whose death was attributed to influenza A infection. The 6-month and 1-year PFS estimates for all patients in stratum A were 74.9% ± 8.2% and 17.8% ± 7.2%, respectively, whereas the 1- and 2-year OS estimates were 43.3% ± 8.7% and 20.0% ± 6.8%, respectively (Figure 4A and B). There was no significant difference in OS distributions between stratum A patients and a historical cohort of patients with newly diagnosed DIPG treated at our institution between October 1992 and May 2011 who met the age criteria for SJPDGF (n = 189 patients) ($P = .99$).[27] Two patients remained alive and free of disease progression for more than 2 years. One of these patients underwent diagnostic stereotactic biopsy, given atypical radiologic findings at presentation, despite exhibiting classic neurologic findings of DIPG. This patient was found to have histone H3 wild-type grade II astrocytoma and is disease-free at 7.5 years from diagnosis. Remarkably, the other patient, who was thought to have clinical and radiologic characteristics consistent with DIPG at diagnosis and who did not undergo diagnostic biopsy, was noted to have diffuse midline glioma, H3 K27M mutant, on biopsy at radiographic progression 6 years from clinical diagnosis. This patient ultimately succumbed to the disease 7 months after initial progression.

No patients in stratum B were lost to follow-up. The 6-month and 1-year PFS estimates for all patients in stratum B were 10.3% ± 5.6% and 5.2% ± 3.5%, respectively, whereas the 1- and 2-year OS estimates were 72.1% ± 9.5% and 33.7% ± 9.7%, respectively (Figure 4C and D). Nine patients experienced clinical progression before cycle 2 of therapy. Only 2 patients received at least 6 cycles of therapy, with one patient completing all 26 cycles. This patient was initially diagnosed with a metastatic temporal anaplastic oligoastrocytoma, despite the lack of chromosomes 1p/19q co-deletion. The tumor was initially managed with subtotal resection and craniospinal irradiation, with local radiographic disease progression noted 4 years later, and was enrolled on SJPDGF. No objective radiologic responses were observed with this therapy, and all patients have died. When compared to patients harboring tumors without *PDGFRA* SNVs and/or CNVs to those with those aberrations, there were no

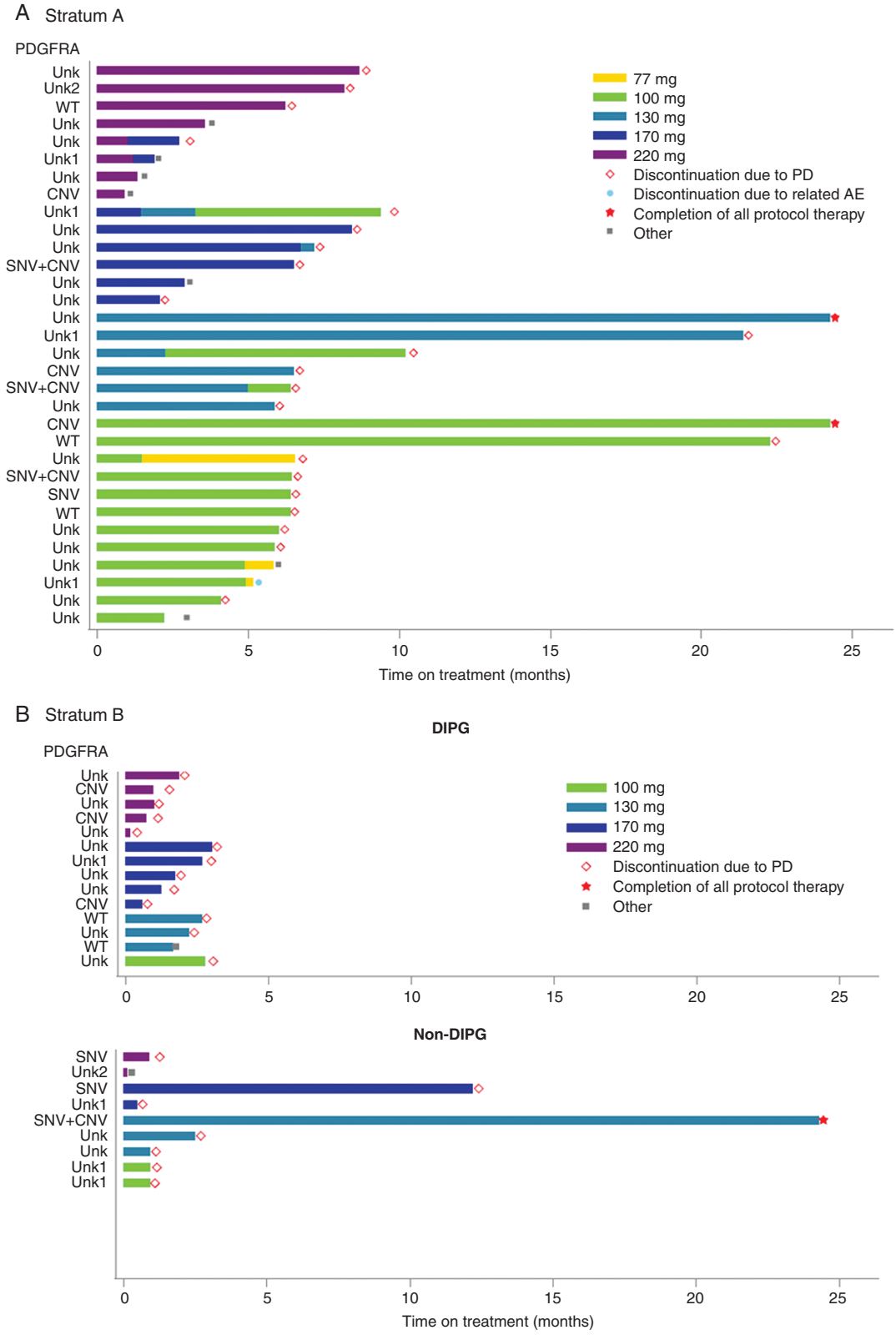

Figure 3. Swimmer plots of treatment duration by *PDGFRA* alteration status in (A) stratum A (newly diagnosed DIPG) and (B) stratum B (recurrent HGG, including DIPG). *PDGFRA* status was defined as the presence of either a somatic nucleotide variant (SNV) or a copy-number variant (CNV), both alterations (SNV + CNV), neither alteration (WT), unknown for both alterations (Unk), unknown for SNVs without an identified CNV (Unk1), and unknown for SNVs with an identified CNV (Unk2). PD, progressive disease; AE, adverse event.

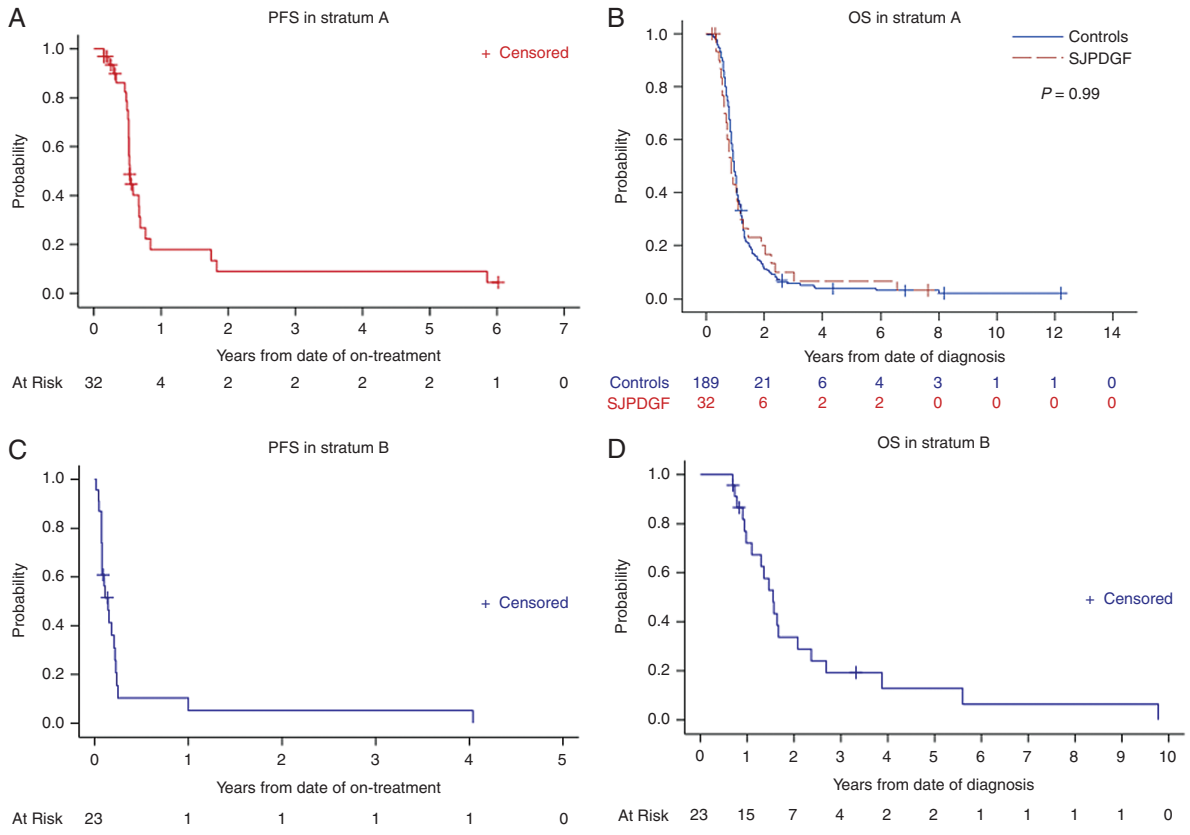

Figure 4. Progression-free survival (PFS) (A) and overall survival (OS) (B) for patients with newly diagnosed DIPG (stratum A) and PFS (C) and OS (D) for patients with recurrent HGG, including DIPG (stratum B). For (B), the OS of a historical control cohort of patients with newly diagnosed DIPG treated at St. Jude Children's Research Hospital from October 1992 to May 2011 who met the age criteria of this clinical trial is presented (n = 189 patients) and compared via the log-rank test.

significant differences in PFS or OS in either stratum (Supplementary Figure 4).

Discussion

In this first-in-pediatrics phase I dose-escalation study of crenolanib in pediatric patients with newly diagnosed DIPG or recurrent HGG, including DIPG, the documented treatment-related AEs were largely consistent with those reported in the phase I study of crenolanib in adults with advanced solid tumors.[11] However, hematologic count suppression, particularly leukopenia, does appear to be unique toxicity in this pediatric population. The most common nonhematologic toxicities observed in stratum A of this study were generally of grades 1 or 2 in severity and consisted of nausea (78%), vomiting (88%), elevated ALT (69%), elevated GGT (63%), elevated AST (69%), proteinuria (59%), hypophosphatemia (59%), hypoalbuminemia (59%), hypermagnesemia (38%), and diarrhea (38%). A similar profile of toxicities and associated intensities was observed in stratum B. As in the adult phase I study, administering 5-HT3 antagonists 30 min before the crenolanib was allowed and crenolanib was taken with food to mitigate nausea and vomiting. These maneuvers were largely effective in limiting the severity of these AEs. Although a film-coated formula of crenolanib was associated with the lowest incidence of treatment-related AEs in adults,[11] coated tablets were not available for this study.

DLTs were similar across strata, and the pediatric MTD established was 170 mg/m^2 for both strata. Importantly, no additional toxicities were identified in stratum A, despite concurrent administration with RT. At this dose, 2 of 6 evaluable patients in stratum A experienced grade 3 elevation of GGT and ALT during the DLT observation period, whereas 2 of 5 evaluable patients in stratum B experienced grade 3 elevation of these liver enzymes plus AST and amylase. Elevated biochemical markers of liver injury were also noted at other dose levels across strata during and after the DLT period, with 28% of patients in stratum A and 17% in stratum B having grade 3/4 elevations of ALT, AST, GGT, or alkaline phosphatase. Although significant elevations of several of these enzymes were noted in adults with advanced solid tumors treated with crenolanib,[11,28] the incidence was lower (<5%), suggesting that the frequency of this gastrointestinal toxicity is distinctive in the pediatric population.

In this pediatric population, crenolanib pharmacokinetics were characterized by slow absorption and elimination and by large interpatient variabilities, which were also observed in adults with advanced cancers receiving crenolanib.[11] The crenolanib half-life of 7.1 h (range, 2.2–18.8 h) in pediatric patients was comparable to the values previously reported in adults of 14 ± 4.2 h.[11] Our analysis also demonstrated that crushing the crenolanib tablet and administering it in applesauce had no effect on crenolanib exposure or C_{MAX} when compared with taking the drug as a whole tablet, which is important when considering a pediatric population. A population-based pharmacokinetic analysis will be performed to quantify further the crenolanib pharmacokinetic variability between patients and determine the influence of patient covariates for potential dosing adjustments. The CNS penetration of crenolanib was assessed in one patient that showed a CSF:total serum ratio of 0.025. In vitro, crenolanib exhibited high protein binding in human plasma with an unbound fraction of 4.1%.[29] Assuming a similar in vivo protein binding, the CSF:unbound serum ratio, a more relevant metric, would be 0.61, suggesting a good CNS penetration for this patient.

To delineate somatic molecular alterations and assess the frequency of *PDGFRA* alterations within these 2 cohorts, we evaluated histone H3 K27M mutation status and *PDGFRA* hotspot mutations and copy-number alterations in those patients who underwent tumor tissue sampling for whom sufficient tissue was available. Consistent with prior reports,[7,30,31] the vast majority of patients (92%) with a clinical diagnosis of DIPG with ultimate histologic evaluation harbored histone H3 K27M mutations, whereas K27M mutation was detected in only 50% of patients in stratum B and was restricted to patients with DIPG. Similarly, *PDGFRA* alterations were observed at rates comparable to those in published reports.[2,6–10] Although the scarcity of tissue sampling and the timing of *PDGFRA* analysis in relation to disease course present obvious challenges when evaluating the impact of *PDGFRA* alteration on crenolanib treatment response and outcomes, we considered this analysis important to a better understanding of the potential utility of crenolanib in this population. Acknowledging this limitation, we observed no obvious correlation with treatment duration in patients with *PDGFRA* alterations, including SNVs and CNV.

To evaluate a preliminary signal of the efficacy of crenolanib in newly diagnosed DIPG, an expansion cohort within stratum A of 6 additional patients treated at the MTD was incorporated into the study. When compared to a historical cohort of 189 similarly matched patients treated at our institution, there was no significant difference in overall survival outcomes ($P = .99$). Acknowledging the limitations of selection bias with regard to tissue sampling, the timing of tissue analysis as discussed above, and the limited sample size, we also observed no significant difference in PFS or OS between those patients with a genetic alteration in *PDGFRA* and those without an alteration across either stratum. Genetic biomarkers associated with response to PDGFR inhibition remain ill-defined, although both amplification and specific activating mutations of *PDGFRA* have been implicated.[2,32–34] The success of precision oncology rests, at least in part, on successfully identifying these biomarkers. Critical steps toward this realization include systematic functional characterization of *PDGFRA* alterations and their impact on the efficacy of available targeted therapies,[35] as well as designing clinical trials that facilitate safe tumor genetic profiling and intratumoral pharmacokinetic and pharmacodynamic assessment in this patient population.[36–38]

In summary, crenolanib demonstrated generally increasing pharmacokinetic exposures with increasing doses. Once-daily administration of an uncoated formulation was well tolerated, with toxicities being generally consistent with those observed in adults. A recommended pediatric phase II dosage of 170 mg/m^2 once daily with food, with or without RT, has been established. Despite this, neither a correlation with *PDGFRA* alterations and outcomes nor a preliminary signal of efficacy was observed. The evaluation of rational combination therapy with crenolanib in models of pediatric HGG[2,3,39] and the development of *PDGFRA* biomarker–driven clinical trials in this patient population (NCT02626364) might be particularly valuable if further clinical investigation of crenolanib is considered, given the temporal and spatial heterogeneity of genetic aberrations of *PDGFRA* and the redundant RTK signaling pathways operating in pHGG.[6,40] To this end, preliminary reports have suggested clinical tolerability and responses to combination therapy with crenolanib and conventional chemotherapy,[41] and crenolanib is currently being evaluated in combination with targeted small molecular inhibitors,[42] including IDH1/2 and BCL-2 inhibitors, as well as in phase III trials in combination with chemotherapy in patients with newly diagnosed acute myeloid leukemia (AML) (NCT03258931) or refractory AML (NCT03250338).

Supplementary material

Supplementary material is available at *Neuro-Oncology Advances* online.

Keywords

crenolanib | diffuse intrinsic pontine glioma | diffuse midline glioma | H3 K27M | pediatric high-grade glioma | phase I clinical trial

Funding

This work was supported in part by Arog Pharmaceuticals, Inc., the American Lebanese Syrian Associated Charities (ALSAC), and the National Cancer Institute (P30 CA021765; St. Jude Cancer Center Support Grant, P01CA096832 to S.J.B. and J.Z.). The content is solely the responsibility of the authors and does not necessarily represent the official views of the National Institutes of Health.

Acknowledgments

We thank the clinical PK nurses and nursing team at St. Jude Children's Research Hospital for assistance in obtaining serum

samples and Keith A. Laycock, PhD, ELS, for scientific editing of the manuscript.

Conflict of interest statement. The authors declare no potential conflicts of interest. C.W. has received research funding for unrelated studies from Eli Lilly and Pfizer; she is presently employed by Neoleukin Therapeutics, Inc.

Authorship statement. Experimental design: A.B., T.E.M., A.O.T., C.F.S., C.W., and A.G.; implementation: C.L.T., A.B., J.C., O.C., J.H., B.A.O., X.L., Z.P., J.Z., S.J.B., T.E.M., V.J., A.O.T., C.F.S., C.W., and A.G.; analysis and interpretation of the data: C.L.T., A.B., J.C., O.C., J.H., B.A.O., J.Z., S.J.B., A.O.T., C.F.S., C.W., and A.G.; writing of the manuscript: C.L.T., A.B., C.W., and A.G.

References

1. Dai C, Celestino JC, Okada Y, Louis DN, Fuller GN, Holland EC. PDGF autocrine stimulation dedifferentiates cultured astrocytes and induces oligodendrogliomas and oligoastrocytomas from neural progenitors and astrocytes in vivo. *Genes Dev.* 2001;15(15):1913–1925.
2. Paugh BS, Zhu X, Qu C, et al. Novel oncogenic PDGFRA mutations in pediatric high-grade gliomas. *Cancer Res.* 2013;73(20):6219–6229.
3. Filbin MG, Tirosh I, Hovestadt V, et al. Developmental and oncogenic programs in H3K27M gliomas dissected by single-cell RNA-seq. *Science.* 2018;360(6386):331–335.
4. Larson JD, Kasper LH, Paugh BS, et al. Histone H3.3 K27M accelerates spontaneous brainstem glioma and drives restricted changes in bivalent gene expression. *Cancer Cell.* 2019;35(1):140–155.e7.
5. Chen CCL, Deshmukh S, Jessa S, et al. Histone H3.3G34-mutant interneuron progenitors co-opt PDGFRA for gliomagenesis. *Cell.* 2020;183(6):1617–1633.e22.
6. Paugh BS, Broniscer A, Qu C, et al. Genome-wide analyses identify recurrent amplifications of receptor tyrosine kinases and cell-cycle regulatory genes in diffuse intrinsic pontine glioma. *J Clin Oncol.* 2011;29(30):3999–4006.
7. Wu G, Diaz AK, Paugh BS, et al. The genomic landscape of diffuse intrinsic pontine glioma and pediatric non-brainstem high-grade glioma. *Nat Genet.* 2014;46(5):444–450.
8. Bax DA, Mackay A, Little SE, et al. A distinct spectrum of copy number aberrations in pediatric high-grade gliomas. *Clin Cancer Res.* 2010;16(13):3368–3377.
9. Barrow J, Adamowicz-Brice M, Cartmill M, et al. Homozygous loss of ADAM3A revealed by genome-wide analysis of pediatric high-grade glioma and diffuse intrinsic pontine gliomas. *Neuro Oncol.* 2011;13(2):212–222.
10. Diaz AK, Baker SJ. The genetic signatures of pediatric high-grade glioma: no longer a one-act play. *Semin Radiat Oncol.* 2014;24(4):240–247.
11. Lewis NL, Lewis LD, Eder JP, et al. Phase I study of the safety, tolerability, and pharmacokinetics of oral CP-868,596, a highly specific platelet-derived growth factor receptor tyrosine kinase inhibitor in patients with advanced cancers. *J Clin Oncol.* 2009;27(31):5262–5269.
12. Heinrich MC, Griffith D, McKinley A, et al. Crenolanib inhibits the drug-resistant PDGFRA D842V mutation associated with imatinib-resistant gastrointestinal stromal tumors. *Clin Cancer Res.* 2012;18(16):4375–4384.
13. Zhang W, Gao C, Konopleva M, et al. Reversal of acquired drug resistance in FLT3-mutated acute myeloid leukemia cells via distinct drug combination strategies. *Clin Cancer Res.* 2014;20(9):2363–2374.
14. Elmeliegy M, Throm SL, Wang F, Bai F, Ramachandran A, Stewart CF. Abstract 2742: Cerebral microdialysis for simultaneous sampling of crenolanib (PDGFR inhibitor) and erlotinib (EGFR inhibitor) in mouse models of glioma. *Cancer Res.* 2012;72:2742.
15. Pollack IF, Jakacki RI, Blaney SM, et al. Phase I trial of imatinib in children with newly diagnosed brainstem and recurrent malignant gliomas: a pediatric brain tumor consortium report. *Neuro Oncol.* 2007;9(2):145–160.
16. Broniscer A, Baker SD, Wetmore C, et al. Phase I trial, pharmacokinetics, and pharmacodynamics of vandetanib and dasatinib in children with newly diagnosed diffuse intrinsic pontine glioma. *Clin Cancer Res.* 2013;19(11):3050–3058.
17. Broniscer A, Jia S, Mandrell B, et al. Phase 1 trial, pharmacokinetics, and pharmacodynamics of dasatinib combined with crizotinib in children with recurrent or progressive high-grade and diffuse intrinsic pontine glioma. *Pediatr Blood Cancer.* 2018;65(7):e27035.
18. Pfeifer H, Wassmann B, Hofmann WK, et al. Risk and prognosis of central nervous system leukemia in patients with Philadelphia chromosome-positive acute leukemias treated with imatinib mesylate. *Clin Cancer Res.* 2003;9(13):4674–4681.
19. Neville K, Parise RA, Thompson P, et al. Plasma and cerebrospinal fluid pharmacokinetics of imatinib after administration to nonhuman primates. *Clin Cancer Res.* 2004;10(7):2525–2529.
20. Lombardo LJ, Lee FY, Chen P, et al. Discovery of *N*-(2-chloro-6-methylphenyl)-2-(6-(4-(2-hydroxyethyl)-piperazin-1-yl)-2-methylpyrimidin-4-ylamino)thiazole-5-carboxamide (BMS-354825), a dual Src/Abl kinase inhibitor with potent antitumor activity in preclinical assays. *J Med Chem.* 2004;47(27):6658–6661.
21. Carter TA, Wodicka LM, Shah NP, et al. Inhibition of drug-resistant mutants of ABL, KIT, and EGF receptor kinases. *Proc Natl Acad Sci U S A.* 2005;102(31):11011–11016.
22. Roberts MS, Turner DC, Owens TS, et al. Determination of crenolanib in human serum and cerebrospinal fluid by liquid chromatography-electrospray ionization-tandem mass spectrometry (LC-ESI-MS/MS). *J Chromatogr B Analyt Technol Biomed Life Sci.* 2013;929:1–5.
23. Rusch M, Nakitandwe J, Shurtleff S, et al. Clinical cancer genomic profiling by three-platform sequencing of whole genome, whole exome and transcriptome. *Nat Commun.* 2018;9(1):3962.
24. Tate JG, Bamford S, Jubb HC, et al. COSMIC: the catalogue of somatic mutations in cancer. *Nucleic Acids Res.* 2019;47(D1):D941–D947.
25. Kaderbhai CG, Boidot R, Beltjens F, et al. Use of dedicated gene panel sequencing using next generation sequencing to improve the personalized care of lung cancer. *Oncotarget.* 2016;7(17):24860–24870.
26. Gomes AL, Gouveia A, Capelinha AF, et al. Molecular alterations of KIT and PDGFRA in GISTs: evaluation of a Portuguese series. *J Clin Pathol.* 2008;61(2):203–208.
27. Jackson S, Patay Z, Howarth R, et al. Clinico-radiologic characteristics of long-term survivors of diffuse intrinsic pontine glioma. *J Neurooncol.* 2013;114(3):339–344.
28. Michael M, Vlahovic G, Khamly K, Pierce KJ, Guo F, Olszanski AJ. Phase Ib study of CP-868,596, a PDGFR inhibitor, combined with docetaxel with or without axitinib, a VEGFR inhibitor. *Br J Cancer.* 2010;103(10):1554–1561.
29. Zimmerman EI, Turner DC, Buaboonnam J, et al. Crenolanib is active against models of drug-resistant FLT3-ITD-positive acute myeloid leukemia. *Blood.* 2013;122(22):3607–3615.
30. Schwartzentruber J, Korshunov A, Liu XY, et al. Driver mutations in histone H3.3 and chromatin remodelling genes in paediatric glioblastoma. *Nature.* 2012;482(7384):226–231.
31. Wu G, Broniscer A, McEachron TA, et al.; St. Jude Children's Research Hospital–Washington University Pediatric Cancer Genome Project.

Somatic histone H3 alterations in pediatric diffuse intrinsic pontine gliomas and non-brainstem glioblastomas. *Nat Genet.* 2012;44(3):251–253.

32. Debiec-Rychter M, Dumez H, Judson I, et al.; EORTC Soft Tissue and Bone Sarcoma Group. Use of c-KIT/PDGFRA mutational analysis to predict the clinical response to imatinib in patients with advanced gastrointestinal stromal tumours entered on phase I and II studies of the EORTC soft tissue and bone sarcoma group. *Eur J Cancer.* 2004;40(5):689–695.
33. Ozawa T, Brennan CW, Wang L, et al. PDGFRA gene rearrangements are frequent genetic events in PDGFRA-amplified glioblastomas. *Genes Dev.* 2010;24(19):2205–2218.
34. Disel U, Madison R, Abhishek K, et al. The pan-cancer landscape of coamplification of the tyrosine kinases KIT, KDR, and PDGFRA. *Oncologist.* 2020;25(1):e39–e47.
35. Ip CKM, Ng PKS, Jeong KJ, et al. Neomorphic PDGFRA extracellular domain driver mutations are resistant to PDGFRA targeted therapies. *Nat Commun.* 2018;9(1):4583.
36. Gupta N, Goumnerova LC, Manley P, et al. Prospective feasibility and safety assessment of surgical biopsy for patients with newly diagnosed diffuse intrinsic pontine glioma. *Neuro Oncol.* 2018;20(11):1547–1555.
37. Pfaff E, El Damaty A, Balasubramanian GP, et al. Brainstem biopsy in pediatric diffuse intrinsic pontine glioma in the era of precision medicine: the INFORM study experience. *Eur J Cancer.* 2019;114:27–35.
38. Mueller S, Jain P, Liang WS, et al. A pilot precision medicine trial for children with diffuse intrinsic pontine glioma-PNOC003: a report from the Pacific Pediatric Neuro-Oncology Consortium. *Int J Cancer.* 2019;145(7):1889–1901.
39. Cenciarelli C, Marei HE, Zonfrillo M, et al. PDGF receptor alpha inhibition induces apoptosis in glioblastoma cancer stem cells refractory to anti-Notch and anti-EGFR treatment. *Mol Cancer.* 2014;13:247.
40. Hoffman LM, DeWire M, Ryall S, et al. Spatial genomic heterogeneity in diffuse intrinsic pontine and midline high-grade glioma: implications for diagnostic biopsy and targeted therapeutics. *Acta Neuropathol Commun.* 2016;4:1.
41. Goldberg AD, Coombs CC, Wang ES, et al. Younger patients with newly diagnosed FLT3-mutant AML treated with crenolanib plus chemotherapy achieve adequate free crenolanib levels and durable remissions. *Blood.* 2019;134:1326.
42. Daver N, Goldberg AD, DiNardo CD, et al. Biomarker driven umbrella trial of crenolanib in combination with ivosidenib, enasidenib, venetoclax, Vyxeos and/or salvage chemotherapy in FLT3 mutant AML. *Blood.* 2020;136:16–17.